ISSN 1870-4069

3D Plant Geometry Understanding Using a CNN-Superpixel Approach

Luis A. Cundapi López[1], Carlos A. Ramírez Mendoza[1], Madain Pérez Patricio[1], German Ríos Toledo[1], J. A. de Jesús Osuna Coutiño[2]

[1] Tecnológico Nacional de México Campus Tuxtla Gutiérrez, Mexico

[2] Instituto Nacional de Astrofísica, Óptica y Electrónica, Mexico

{m13270146, m14270620, german.rt}@tuxtla.tecnm.mx, madain.pp@tuxtla.edu.mx, osuna@inaoep.mx

Abstract: Plant stress phenotyping consists of identification, classification, quantification, and prediction (ICQP) in crop stress. There are several approaches to plant stress identification. However, most of these approaches are based on the use of expert employees or invasive techniques. In general, expert employees have a good performance on different plants, but this alternative requires sufficient staff in order to guarantee quality crops. On the other hand, invasive techniques need the dismemberment of the leaves. To address this problem, an alternative is to process an image seeking to interpret areas of the images where the plant geometry may be observed, thus removing the qualified labor dependency or the crop dismemberment, but adding the challenge of having to interpret images ambiguities correctly. Motivated by the latter, we propose a new CNN-Superpixel approach for plant stress phenotyping. This strategy combines the abstraction power of deep learning and the information that provides the plant geometry. For that, our methodology has three steps. First, the plant recognition step provides the segmentation, location, and delimitation of the crop. Second, we propose a leaf detection analysis to classify and locate the boundaries between the different leaves. Finally, we use a depth sensor and the pinhole camera model to extract a 3D reconstruction.

Keywords: Plant geometry understanding, plant stress phenotyping, CNN, superpixel, deep learning.

1 Introduction

Phenotype is the observable characteristics or traits of an organism that are produced by the interaction of the genotype (the genetic constitution of an organism) and the

environment [1]. Understanding these processes that span plant's lifetime in a permanently changing environment is essential for the advancement of basic plant science [22]. Plant phenotyping is an important tool to address and understand plant environment interaction and its translation into application in crop management practices [27]. Abiotic stress includes factors such as drought, flood, salinity, radiation, high and low temperatures, among others.

Meanwhile, in biotic stress, pathogens such as bacteria, fungi, yeasts, worms (nematodes) are considered. Current approaches for accurate classification of biotic and abiotic stresses in crop research and production are predominantly visual and require specialized training. However, these techniques are subject to subjectivity and the experience of the people who perform them. In addition, the availability of visual signals allows the identification of types of stress, but these visual signals do not coincide with the symptoms determined by experts [8]. Recently, high-throughput stress phenotyping techniques have been introduced that rely primarily on remote sensing or imaging.

They are able to directly measure morphological traits, but measure physiological parameters mainly indirectly. Plant stress phenotyping is divided into four broad categories, the so-called ICQP paradigm, the acronym represents Identification, Classification, Quantification and Prediction. These four categories naturally fall into a continuum of feature extraction where increasingly more information is inferred from a given image [25].

Depending on the data acquisition devices, Plant Stress Phenotyping can be carried out in two ways: Aerial and Ground Based Sensing. The rapid development of image-based phenotyping methods based on ground-operating devices or Unmanned Aerial Vehicles (UAV) has increased our ability to evaluate traits of interestfor crop breeding in the field [10].

Studies on plant stress include those on drought stress [4], heat stress [26], salt stress [14], nutrient deficiency [18] and and biotic stress [8].

Conventional plant stress identification and classification have invariably relied on human experts identifying visual symptoms as a means of categorization [9]. According to Naik *et al*. [17], current methods for phenotypically measuring are completely visual and labor-intensive.

Naik and his collaborators reported that visual scoring is the simplest, subjective measurement that requires relatively less labor. However, it has reduced accuracy if the evaluation is made in diverse environments and by different raters [24]. Today, determination of crop stress factors using visible symptoms is still often a manual and complex task predominantly carried out by trained and experienced individuals, such as agronomists, crop scientists and plant pathologists [12].

The manual process is laborious, time-consuming and not always reproducible due to the inherently subjective nature of manual ratings, experience and interpretation [8]. It should be noted that the experience over the years is an invaluable resource. Thus, human experts can incorporate their knowledge into automated processes to improve the efficiency of these types of systems.

In the last decades, several sensors and computer vision tools have been developed and became pivotal for quantifying plant traits with increasing throughput and accuracy

[1] https://www.merriam-webster.com/dictionary/phenotype

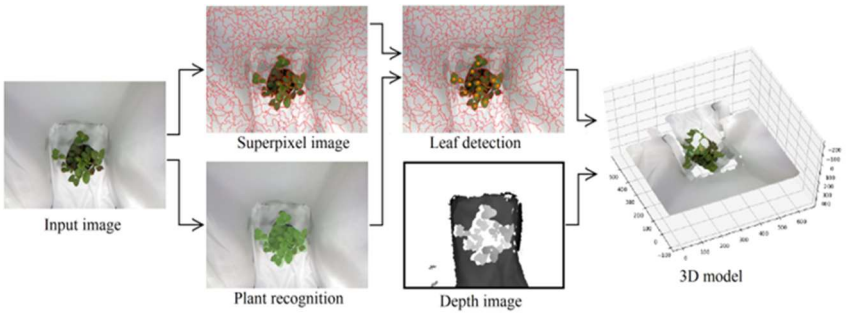

Fig. 1. Block diagram of the proposed methodology.

[22]. Computer vision is a non-contact and non-destructive sensing technology that enables multi-dimensional sensing capabilities [6].

This technology can be used to extract information from a targeted object including morphological (size, shape, texture), spectral (colour, temperature, moisture), and temporal data (growth rate, development,dynamic change of spectral and morphological states) [11]. For commercial production systems, it is more advantageous to develop a real-time plant canopy health, growth and quality monitoring system with multi-sensor platforms.

This can be achieved by a sensing system equipped with a multisensor platform moving over the canopy and ultimately using plants as 'sensors' to communicate their true status and needs [11].

Unlike conventional methods, optical imaging is advanced to measure changes caused by abiotic or biotic stressors in the plant physiology rapidly and without contact. In general, the common imaging technologies have been employed for detecting the crop stress, including digital, fluorescence, thermography, LIght Detection and Ranging(LIDAR), multispectral and hyperspectral imaging techniques [7].

Remote sensing phenotyping methods are non-destructive and non-invasive approaches [23], based mostly on the information provided by visible/near-infrared radiation reflected (or transmitted) and far-infrared(thermal) radiation emitted by the crop. Remote sensing techniques maybe deployed in situ screening for a wide range of breeding objectives,including yield potential, adaptation to abiotic (water stress, extreme temperatures, salinity) and biotic (susceptibility to pests and diseases) limiting conditions, and even quality traits [1].

Another way to measure the state of health or stress of a plant is by using laboratory techniques such as Kjeldahl method [3], a method developed for determining the nitrogen contents in organic and inorganic objects.

For example, this method was applied in [28] to measure the total nitrogen content in samples of rice plants. Kjeldahl method is the most accurate and also the most time-consuming method [19]. Also, it is invasive method since its use implies the destruction of the samples. However, it is useful in investigations where a baseline is required. Thus, it is possible to measure the efficiency of a non-invasive method such as remote-sensing technology.In recent work, there is significant progress in crop stress diagnosis

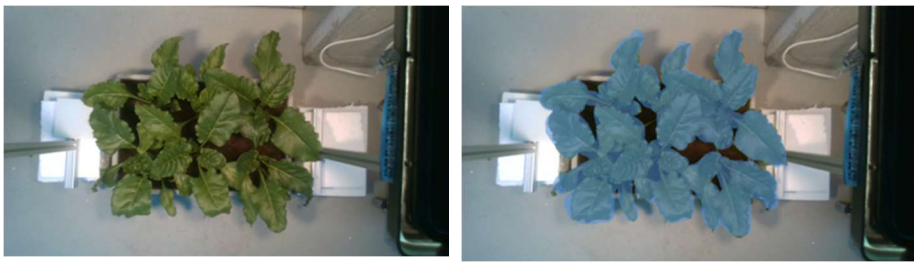

Fig. 2. (a) RGB image; (b) Semantic image.

using machine learning [2]. This was achieved via learning algorithms that learn the relationship between visual appearance and plant stress phenotyping.

Unlike the other trends (using expert employees or invasive techniques), this approach analyzes the plant without qualified labor dependency or the crop dismemberment, but adding the challenge of having to interpret images ambiguities correctly.

Water stress is one of the main causes of death in plants, it occurs in plants in response to a low water environment, where the transpiration rate exceeds the intake of water. The problem of identifying stress in plants has been extensively studied. However, the studies carried out use two-dimensional information to classify the state of a plant, posing the problem of having to extract additional information, with a range of possibilities to obtain better stress analysis results. Other works carry out stress analysis with three-dimensional models for the extraction of the plant, but use rotating tables or a set of images of different poses for its reconstruction.

To address this problem, the contribution of our work is a methodology for the extraction of a 3D model from a single image, this strategy combines the power of abstraction of deep learning and the information provided by the geometry of the plant. For this, we consider 2D and 3D information to predict the effect of water stress on growth caused by deficit of water and nutrients. Section 2 presents the proposed methodology carried out for the extraction of the 3D model and the experiments carried out, in section 3 presents the results for the evaluation of the proposed method. Finally, the results are discussed in section 4.

2 Proposed Methodology

Our methodology has three steps. First, the plant recognition step provides the segmentation, location, and delimitation of the crop. Second, we propose a leaf detection analysis to classify and locate the boundaries between the different leaves. Finally, we use a depth sensor and the pinhole camera model to extract the 3D pose. The schematic representation of the proposal is shown in Figure 1.

2.1 Input Image

We denote the RGB input image as I_p. We divide the image I_p into a grid Θ. The grid Θ consists of sections Θ_w, where w denotes the w-th section in Θ, and each Θ_w

section has a patch $\vartheta_{\varphi,\omega}$. A patch $\vartheta_{\varphi,\omega}$ is a finite set of pixels $\vartheta_{\varphi,\omega} = \{x_1, \ldots, x_u\}$, $\vartheta_{\varphi,\omega} \in \Theta$, where φ and ω are the abscissa and ordinate from the Θ grid, respectively. Pixel $\rho_{\varphi,\omega}$ is a pixel within the patch $\vartheta_{\varphi,\omega}$.

2.2 Plant Recognition

We use a CNN architecture to segment the pixels with a semantic of crop elements. This CNN learns two labels on crops (plant v^1 and no-plant v^2). Although the no-plant label does not correspond to a plant element; we use this label since we need to remove it for the next steps.

2.2.1 Training Set

In the training set of semantic segmentation, we use the "Eschikon Plant Stress Phenotyping Dataset" [13]. This dataset has spatiotemporal-spectral data pertaining to sugarbeet crop growth under no, drought, fertilizer, and weed stress conditions over two months. To obtain the training set, we divide the images of the datasets with labels (plant v^1 and no-plant v^2) in RGB images of 32×32 pixels. For example, we can obtain 630 small sections (32×32 pixels) using an image (1920×1080 pixels).

2.2.2 CNN for Semantic Segmentation

The input of the CNN is an RGB section Φ^i with a size of 32×32 pixels. In this case, we train the YOLOv4 network to learn two labels of crops (plant v^1 and no-plant v^2). Also, our program uses a sliding window with a sweep of one pixel [20]. For that, this program analyzes RGB sections of 32×32 pixels. The CNN paints the central pixel $\rho_{\varphi,\omega}$ of the analyzed RGB section (32×32 pixels). For that, the CNN paints the central pixel $\rho_{\varphi,\omega}$ of the analyzed RGB section $\vartheta_{\varphi,\omega}$ with green color if it has a plant label v^1 (See Figure 2.6). On the other hand, the CNN paints the central pixel $\rho_{\varphi,\omega}$ of the analyzed RGB section $\vartheta_{\varphi,\omega}$ with black color if it has a no-plant label v^2.

2.3 Superpixel Image

We denote the superpixel image as I_s. For the superpixel image I_s, we use the SLIC superpixel approach [19]. The purpose was to classify and locate the boundaries between the different sheets, this algorithm grouped pixels based on their similarity in color and proximity in the image plane. Where ψ_i denotes the i^{th} superpixel in an image I_s. Given an RGB image, it is first converted to the LAB color space to group pixels based on their color similarity and proximity in the image plane, improving discrimination between foreground and background sheets.

This algorithm takes as input a desired number of super pixels K of approximately the same size that is used to segment the input image with super pixels.

For the superpixel approach, we use the following parameters: desired number of superpixels = 999, number of pixel-level iterations = 9, and shape smoothing term = 5. The value of K depends on the type of images being worked on, considering the number

Table 1. Confusion matrix dataset strawberry.

		Predicted label	
		Plant	No-plant
True label	Plant	45,845	4,155
	No-plant	2,522	47,478

of objects that exist in the image, a high number of superpixels is used, in this way the algorithm allows to better locate the edges of the sheets.

The assignment and update steps are repeated until the error converges [5], but we found that 9 iterations are sufficient for the images and using K = 999, greater visualization of details is highlighted.

2.4 Leaf Detection

We use the Hough transform for the leaf detection step. We implement Hough transform to find circles in an image. For that, the Eq. 1 provides the mathematical representation of the circle. Where (a, b) is the center of the circle, and r is the radius in a fixed point (x, y). In this case, the Hough transform locates circles into the superpixel edge of our semantic segmentation. Finally, the detected circles are the leaves of the plant:

$$(x - a)^2 + (y - b)^2 = r^2. \quad (1)$$

2.5 Depth Image

Nowadays, depth-sensing technologies are widely used to scan environments or simplify challenging tasks such as object detection, pose estimation, visual tracking, among others. In this work, we use a Kinect sensor to obtain the plant depth information. For that, we denoted the depth image as D_ε. For the Kinect, we use the following parameters: image resolution= 640×480, frames per second = 12, and maximum depth = 4 meters.

2.6 3D Model Analysis

We use the basic pinhole model to extract the 3D model. This model considers the projection of a point $P(X, Y, Z)$ in space to a point $p(x, y)$ in the image plane. The relative size of an object in the image depends on the image plane distance Z and the focal length f. The focal length f is the distance between the camera center C_o (camera lens center) to the image plane. The optical center or principal point O_o is the origin of coordinates in the image plane, but in practice, it may not be. By similar

triangles, one quickly computes that the point $P(X,Y,Z)$ is mapped to the point $p(fX/Z, fY/Z, f)$ on the image plane.

We use the pinhole model with the image plane information and the depth of the sensor to compute the 3D recovery in crops. In our extraction, we convert the information in meters. For that, we divided the scale factor k with the maximum RGB value (255) and multiplied by a depth z (Subsubsection 2.5). The scale factor k is the maximum depth of the Kinect sensor (Subsubsection 2.5). For example, considering a maximum depth k of 4 meters and a depth estimation z of 128 in grayscale, Z is approximately 2 meters. The Eq. 2-4 compute the coordinates (X,Y,Z) of a point in the space:

$$Z = \frac{k \cdot z}{255}, \tag{2}$$

$$X = \frac{x \cdot Z}{f}, \tag{3}$$

$$Y = \frac{y \cdot Z}{f}. \tag{4}$$

Finally, using the 3D plant model, we calculate the 3D centroid of the detected leaves (Subsubsection 2.4). This centroid provides a 3D compact representation of the leaf. For that, we use a simplification of the intensity centroid. This simplification of intensity centroid obtains the central point by 3D leaf extracted. Defining the moments as:

$$m^j_{p,q,g} = \sum_{X,Y,Z}^{w} X^p Y^q Z^g, \tag{5}$$

where j denotes the j^{th} 3D leaf extracted, and w is the number of pixel projections by leaf. On the other hand, (p,q,g) are the orders of the moment $m^j_{p,q,g}$ (we use an order of 0 or 1). Finally, we determined the intensity centroid as:

$$C^j = \left(\frac{m^j_{1,0,0}}{m^j_{0,0,0}}, \frac{m^j_{0,1,0}}{m^j_{0,0,0}}, \frac{m^j_{0,0,1}}{m^j_{0,0,0}} \right). \tag{6}$$

2.7 Crop Irrigation and Fertigation

The experiment and acclimatization of the plants was carried out in a prototype built with a drip irrigation system with average conditions of temperature of 20 ° C and relative humidity of 60%. The prototype automatically controls 4 12v water pumps with a power of 19 watts and a current of 1A, and 2 incandescent lamps of 150 watts through a mobile application. The lamps were turned on daily from 6:00 a.m. to 6:00 p.m. and the pumps were activated at 8:00 p.m. Twelve strawberry plants organized in four groups called A, B, C and D, each with 3 plants, were placed in the prototype. Groups A and B were used to simulate stress conditions due to lack of water, while C and D were used to simulate stress conditions due to lack of nutrients. Group A was watered with a dose of 250 ml of water and group B with 150 ml of water every 2 days.

Table 1. Semantic segmentation evaluation.

N. images	Dataset sugarbeet			Dataset strawberry		
	Precision	Recall	F1-score	Precision	Recall	F1-score
15,000	0.75	0.78	0.76	0.80	0.85	0.82
20,000	0.78	0.80	0.78	0.85	0.91	0.87
25,000	0.83	0.85	0.83	0.90	0.93	0.91
30,000	0.85	0.90	0.87	0.91	0.93	0.91
40,000	0.88	0.93	0.90	0.91	0.94	0.92
50,000	0.91	0.94	0.92	0.93	0.95	0.93

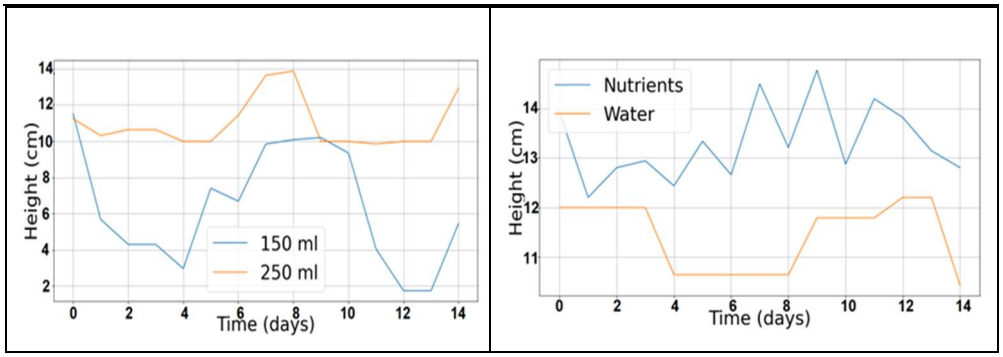

Fig. 3. (a) Water stress grid ; (b) Nutrient stress grid.

Table 2. 3D model evaluation.

RMS(x)	RMS(y)	RMS(z)	Average
0.013416	0.029814	0.007843	0.03697

The plants of group C were watered with 250 ml of water and a 17% nutrient mixture (nitrogen, phosphorus and potassium) and the plants of group D were watered only with 250 ml of water.

In the works related to water stress in plants, the observation period of the experiments is concluded when the plant shows symptoms of wilting causing discoloration or dryness in the leaves, in this way the loss of the studied crop is avoided [15]. Therefore, our observation period for both experiments was 15 days, since in later days the plants showed wilting.

To collect the images in color (RGB) and depth, a Kinect sensor placed at a distance of 90 cm above the foliage of the plants was used. The capture of images was carried out during the 15 days at 1:00 p.m. due to the lighting conditions.

A daily image was taken of a total of 12 plants, this because the plant's reaction to stress took at least one day, in this way 180 images were obtained with a resolution of 640x480 pixels.

3 Results

The problem was addressed as a binary classification problem (*plant* and *no-plant* classes), the positive class was *plant*. Binary classifier predicts the instances of the test set as positive or negative and produces four outcomes: True Positive (TP), True Negative (TN), False Negative (FN) and False Positive (FP). Table 1 shows the results obtained in each prediction made by CNN training with 50,000 sections of 32x32 pixels in each class. It is observed that the network correctly predicted 45,845 sections, 92% of the total of the plant class, as parts that corresponded to the leaf and 47,478 sections, 95% of the total of the non-plant class, were correctly detected.

We use two different datasets to evaluate semantic segmentation ("Eschikon Plant Stress Phenotyping" dataset [13] and a proposed dataset). The proposed dataset was obtained from strawberry plants with 180 images with a resolution of 640x480 pixels. Table 2 shows the result of training the network with different amounts of images.

In it, the metrics are compared according to the recognition and segmentation obtained by CNN in the image sets, obtaining better results with ours. Experiments with 50,000 images showed the highest segmentation and detection precision in the leaves of the plant.

Figure 3 two different graphs are observed that show the behavior of the groups of plants from the applied irrigation, these heights were obtained from the 3D model. Figure 3 a) shows the heights of the plants watered with water in 2 different doses (250 ml and 150 ml) are shown.

The height of the leaves is measured relative to the ground. The better the plant is watered, the more the height of the leaves increases. This can be observed in the group that was watered with the 250 ml dose, the height remains constant or increases up to 2 centimeters, but its height never decreases.

Figure 3 b) shows a comparison of heights between a group of plants irrigated with nutrients and another group irrigated only with water, both groups with 250 ml.

It is observed that the height increases as a function of the soil as the days go by when a plant is watered with enough nutrients that help the plant to grow. By irrigating the plants only with water, they maintain their normal development, however the height of their leaves is maintained or even decreased.

The mean square error (RMS) determines how much the actual data differs from the predictions made by a model. Table 3 shows the RMS obtained by comparing the centroids (X, Y, Z) of the ground truth with respect to the centroids (X, Y, Z) of the CNN.

4 Conclusions

In this work, we have introduced a new CNN-Superpixel approach for 3D plant geometry understanding. Our strategy was to divide and simplify the 3D plant extraction process.

This strategy combines the abstraction power of deep learning and the information that provides crop geometry. For that, our methodology has three steps. First, the plant recognition step provides the segmentation, location, and delimitation of the crop. Second, we propose a leaf detection analysis to classify and locate the boundaries

between the different leaves. Third, we use a depth sensor and the pinhole camera model to extract a 3D reconstruction.

The quantitative experiments were conformed of the plant recognition (semantic segmentation) and its 3D extraction. In the recognition evaluation, we used two datasets that provide different crops ("Eschikon Plant Stress Phenotyping" dataset [?] and a proposed dataset). For that, we analyzed two labels of crops (plant and no-plant).

For example, our plant segmentation had an average $recall$ of 0.945, i.e., considering the ground-truth, we recognized 94.5%. On the other hand, the plant segmentation had an average $precision$ of 0.92, i.e., considering the semantic segmentation, we segmented 92.0% correctly. The segmentation is fundamental since the plant recognition is proportional to the precision of 3D extraction on the (X,Y) axis of the 3D model.

Finally, for the 3D plant extraction evaluation, we use our proposed dataset. We used the RMS error for the quantitative evaluation.

The Mean Square Error (RMS) determines how much the actual data differs from the predictions made by a model. For that, we compared the centroids (X, Y, Z) of each leaf in the 3D model of the ground truth with our centroids (X, Y, Z).

In this experiment, we have an average RMS error (Z) of 0.007843, i.e., an error of 0.007 centimeters in 4 meters. On the other hand, considering the coordinates (X, Y, Z) in the extraction, we had an average RMS (X, Y, Z) of 0.03697.

References

1. Ali, A. A.: Maize productivity in the new millennium. Hassan Awaad, MohamedAbu-hashim, Abdelazim Negm (editors), pp. 509 (2021)
2. Anami, B. S., Malvade, N. N., Palaiah, S.: Classification of yield affecting biotic andabiotic paddy crop stresses using field images. Information Processing in Agricul-ture, vol. 7, no. 2, pp. 272–285 (2020)
3. Bellomonte, G., Costantini, A., Giammarioli, S.: Comparison of modified automaticdumas method and the traditional kjeldahl method for nitrogen determination ininfant food. Journal of the Association of Official Analytical Chemists, vol 70, no. 2, pp. 227–229 (1987)
4. Clauw, P., Coppens, F., De Beuf, K., Dhondt, S., van Daele, T., Maleux, K., Storme, V., Clement, L., Gonzalez, N., Inze, D.: Leaf responses to mild droughtstress in natural variants of arabidopsis. Plant physiology, vol. 167, no. 3, pp. 800–816 (2015)
5. Derksen, D., Inglada, J., Michel, J.: Scaling up slic superpixels using a tile-basedapproach. IEEE Transactions on Geoscience and Remote Sensing, vol. 57, no. 5, pp. 3073–3085 (2019)
6. Elvanidi, A., Zinkernagel, J., Max, J., Katsoulas, N.: Contribution of hyperspec-tral imaging to monitor water content in soilless growing cucumber crop. In: International Symposium on Advanced Technologies and Management for Innovative Greenhouses: GreenSys2019, 1296. pp. 1055–1062 (2019)
7. Gao, Z., Luo, Z., Zhang, W., Lv, Z., Xu, Y.: Deep learning application in plantstress imaging: A review. AgriEngineering, vol. 2, no. 3, pp. 430–446 (2020)
8. Ghosal, S., Blystone, D., Singh, A. K., Ganapathysubramanian, B., Singh, A.,Sarkar, S.: An explainable deep machine vision framework for plant stress phe-notyping. In: Proceedings of the National Academy of Sciences, vol. 115, no. 18, pp. 4613–4618 (2018)
9. Joalland, S., Screpanti, C., Varella, H. V., Reuther, M., Schwind, M., Lang, C.,Walter, A., Liebisch, F.: Aerial and ground based sensing of tolerance to beet cystnematode in sugar beet. Remote Sensing. vol. 10, no. 5, pp. 787 (2018)

10. Katsoulas, N., Elvanidi, A., Ferentinos, K. P., Kacira, M., Bartzanas, T., Kittas, C.: Crop reflectance monitoring as a tool for water stress detection in greenhouses: A review. Biosystems Engineering, vol. 151, pp. 374–398 (2016)
11. Khanna, R., Schmid, L., Walter, A., Nieto, J., Siegwart, R., Liebisch, F.: A spatiotemporal spectral framework for plant stress phenotyping. Plant methods, vol. 15, no. 1, pp. 1–18 (2019)
12. Kirchgessner, N., Liebisch, F., Yu, K., Pfeifer, J., Friedli, M., Hund, A., Walter, A.: The ETH field phenotyping platform fip: A cable-suspended multi-sensor system. Functional Plant Biology, vol. 44, no. 1, pp. 154–168 (2016)
13. Liñan-Vigo, F. N.: Plasticidad fenotípica en plantas de origanum vulgare "ni-gra"(orégano) en respuesta al estrés hídrico en condiciones de invernadero (2018)
14. Luna-Flores, W., Estrada-Medina, H., Jimenez-Osornio, J., Pinzon-Lopez, L.: Effect of water stress on growth and water use efficiency of tree seedlings of threedeciduous species. Terra Latinoamericana, vol. 30, no. 4, pp. 343–353 (2012)
15. Naik, H. S., Zhang, J., Lofquist, A., Assefa, T., Sarkar, S., Ackerman, D., Singh, A., Singh, A. K., Ganapathysubramanian, B.: A real-time phenotyping frame work using machine learning for plant stress severity rating in soybean. Plant methods, vol. 13, no. 1, pp. 1–12 (2017)
16. Neilson, E. H., Edwards, A. M., Blomstedt, C., Berger, B., Møller, B. L., Gleadow, R. M.: Utilization of a high-throughput shoot imaging system to examine the dy-namic phenotypic responses of a c4 cereal crop plant to nitrogen and water defi-ciency over time. Journal of experimental botany, vol. 66, no. 7, pp. 1817–1832 (2015)
17. Ning, Y., Zhang, H., Zhang, Q., Zhang, X.: Rapid identification and quantitative pitmud by near infrared spectroscopy with chemometrics. Vibrational Spectroscopy vol. 110, pp. 103–116 (2020) doi.org/10.1016/j.vibspec.2020.103116
18. Nowosad, J., Stepinski, T.: Generalizing the simple linear iterative clustering (slic) superpixels (2021)
19. Osuna-Coutiño, J. A. D J., Martinez-Carranza, J.: Volumetric structure extraction in a single image. The Visual Computer, Springer (2021) doi: 10.1007/s00371-021-02163-w
20. Pieruschka, R., Schurr, U.: Plant phenotyping: Past, present, and future. Plant Phenomics 2019 (2019) doi: 10.34133/2019/7507131
21. Rist, F., Gabriel, D., Mack, J., Steinhage, V., Topfer, R., Herzog, K.: Combination of an automated 3d field phenotyping workflow and predictive modelling forhigh through put and non-invasive phenotyping of grape bunches. Remote Sensing, vol. 11, no. 24, pp. 2953 (2019)
22. Rodriguez de Cianzio, S., WR, F., Ic, A.: Genotypic evaluation for iron deficiency chlorosisin soybeans by visual scores and chlorophyll concentration (1979), 24. Singh, A.K., Ganapathysubramanian, B., Sarkar, S., Singh, A.: Deep learning forplant stress phenotyping: trends and future perspectives. Trends in plant science, vol. 23, no. 10, pp. 883–898 (2018)
23. Vasseur, F., Bontpart, T., Dauzat, M., Granier, C., Vile, D.: Multivariate genetic analysis of plant responses to water deficit and high temperature revealed con-trasting adaptive strategies. Journal of experimental botany, vol. 65, no. 22, pp. 6457–6469 (2014)
24. Walter, A., Finger, R., Huber, R., Buchmann, N.: Opinion: Smart farming is keyto developing sustainable agriculture. In: Proceedings of the National Academy of Sciences, vol. 114, no. 24, pp. 6148–6150 (2017)
25. Wang, Y., Wang, D., Zhang, G., Wang, J.: Estimating nitrogen status of rice usingthe image segmentation of gr thresholding method. Field Crops Research, vol. 149, pp. 33–39 (2013)